ELSEVIER

Journal of Nuclear Materials 307–311 (2002) 966–970

journal of nuclear materials

www.elsevier.com/locate/jnucmat

# Evolution of a defect structure of Pd–Ag alloys during tritium exposure

V. Tebus [*], L. Rivkis, E. Dmitrievskaia, G. Arutunova, I. Golikov, N. Ryazantseva, V. Filin, V. Kapychev, V. Bulkin

*Federal State Unitarian Enterprise, A.A. Bochvar Research Institute of Inorganic Materials (VNIINM), P.O. Box 369, Moscow 123060, Russia*

## Abstract

Pd–Ag alloys, a material for palladium diffuser of the ITER fuel clean-up system, were investigated after long-term usage exposition in tritium. Nucleation and evolution of the alloy structure defects as a result of a radiogenic helium-3 accumulation have been examined using electron microscopy, positron annihilation and X-ray analysis. The types of helium containing defects and their characteristics were determined. The early stage of helium bubbles forming was observed. It was shown that the simple defect concentration decreased slowly and helium-3 bubble sizes and concentration increased during the tritium exposure.

## 1. Introduction

Pd–Ag alloys are considered as a material for palladium diffuser of the ITER fuel clean-up system. Isotropic non-destructive He-3 formation in palladium alloys takes place due to tritium decay by the reaction $T \rightarrow He^3 + \beta$ during diffuser exploitation. It is proposed that the He-3 accumulation may be as large as 2000 appm after a 3 year exploitation of the diffuser at working temperature 350–400 °C and D-T mixture pressure $\simeq 10^5$ Pa. Experimental data from publications [1–4] are not enough to describe the structure changes in the alloys under such conditions.

The results of our investigation of the degradation probability of the Russian industrial Pd–Ag alloy V-1 (Pd 15Ag 0.6Pt 0.6Ru 1.0Au 0.2Al) properties during long-time exposure to tritium at 350 °C were published earlier [5–7]. Now we present the results of an investigation on the structure changes of this alloy under 400 °C.

## 2. Experimental method

He-3 accumulation in V-1 tube specimens ($\varnothing$ 1.2 × 0.1 mm$^2$) was reached by immersion in a D–T gas mixture at the following conditions: immersion temperature 350 and 400 °C; immersion pressure 0.8–0.9 MPa; immersion medium D–T (1:1) gas mixture. The experimental device was described earlier [5].

To prevent the effects connected with the $\alpha \rightarrow \beta$ transformation in palladium hydride the evacuated container with the specimens was heated up to the immersion temperature (higher 300 °C) prior to D–T mixture filling. The D–T mixture was taken to getter at the end of each stage of the experiment and the container with the specimens was evacuated prior to lowering the temperature.

The following investigations were done using tritium exposure specimens: electron microscopy, positron annihilation spectroscopy, X-ray structure analysis and stress–strain tests. The He-3 formation rate was taken as $6.4 \times 10^{-6}$ He atom/T atom per hour. The estimated

---

[*] Corresponding author. Tel.: +7-095 190 8352; fax: +7-095 196 4168.

*E-mail address:* tebus@bochvar.ru (V. Tebus).

0022-3115/02/$ - see front matter © 2002 Elsevier Science B.V. All rights reserved.
PII: S0022-3115(02)01302-8

Table 1
Estimated He-3 concentrations in the alloy

| Tritium exposure (h) | $He^3$ concentration (appm) |
|---|---|
| *Immersion temperature 350 °C* | |
| 385 | 73 |
| 938 | 205 |
| 1458 | 330 |
| 2004 | 470 |
| *Immersion temperature 400 °C* | |
| 737 | 140 |
| – | – |
| 1552 | 270 |
| 2300 | 500 |

helium concentrations in the alloy after each stage of the experiment are represented in Table 1.

## 3. Experimental results

Alloy microstructure changes during tritium exposure are represented in Figs. 1–4. The specimen analysis data treatment is represented in Tables 2–5.

The program and methods, well known from literature [8–14], were used for handling of positron annihilation spectroscopy data. Helium bubble parameters were estimated assuming that the bubbles were in an equilibrium state. The microstructure of initial specimens is typical for deformed material. There are high concentrations of dislocations, which form loop structure with characteristic grid size 40–100 nm. During the D–T exposure the gradually recrystallization of the alloy was accompanied by the fine grain structure formation from the dislocation grid. He-3 bubbles were uniformly distributed through the grain volume; no primary bubble concentration growth along grain boundaries and dislocations was observed. The influence of D–T exposure on tensile properties of the V-1 alloy is represented in Table 5.

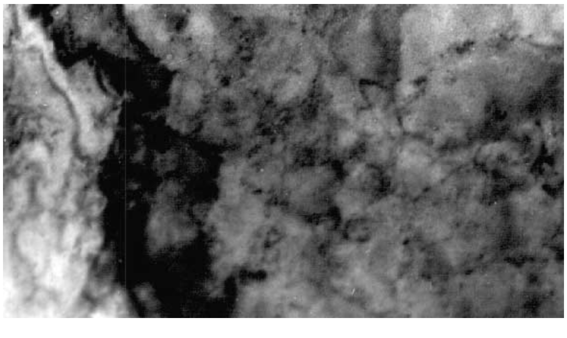

Fig. 1. Microstructure of the 470 appm He-3 content specimen (350 °C).

Fig. 2. Microstructure of the 140 appm He-3 content specimen (400 °C).

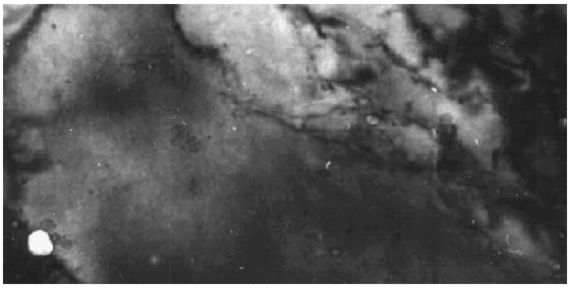

Fig. 3. Microstructure of the 270 appm He-3 content specimen (400 °C).

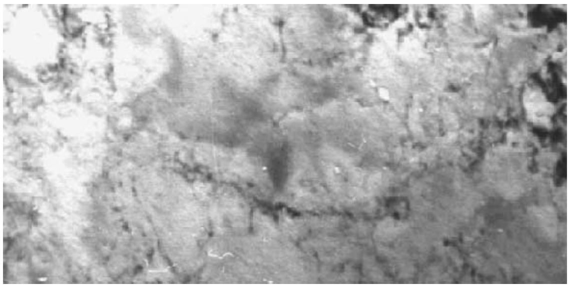

Fig. 4. Microstructure of the 500 appm He-3 content specimen (400 °C).

## 4. Discussion

In our previous publications [6,7] the following mechanism was proposed for V-1 alloy structure changes during the D–T exposure at 350 °C. At first the formation of the radiogenic helium solid solution takes place. Only a minor helium amount is presented in He–V clusters (not higher than 8% from its content in the alloy). The gradual destruction of the solid solution occurs as the exposure prolonged. The simultaneous growth of He–V clusters and the nucleation of He-3 bubbles accompany this process. The whole He-3 excess

Table 2
Lattice parameter changes during tritium exposure

| He$^3$ concentration (appm) | Lattice parameter, $a$ (nm) | $\Delta a/a$ (%) |
|---|---|---|
| *Immersion temperature 350 °C* | | |
| 0 (initial) | 0.3913 | – |
| 73 | 0.39155 | 0.07 |
| 205 | 0.39150 | 0.05 |
| 330 | 0.39150 | 0.05 |
| 470 | 0.39140 | 0.02 |
| *Immersion temperature 400 °C* | | |
| 0 (initial) | 0.3913 | – |
| 140 | 0.3916 | 0.07 |
| 270 | 0.3918 | 0.12 |
| 500 | 0.3916 | 0.07 |

Table 3
He–V clusters and helium bubbles evolution from positron annihilation spectroscopy data

| He$^3$ concentration (appm) | Cluster composition (bubble size, nm) | Cluster (bubbles) concentration (s m$^{-3}$) |
|---|---|---|
| *Immersion temperature 350 °C* | | |
| Initial | V | $1.1 \times 10^{17}$ |
| | 2V | $1.1 \times 10^{17}$ |
| 73 | 2V–2(3)He | $3.7 \times 10^{16}$ |
| | 2V–He | $1.7 \times 10^{17}$ |
| | or 5V–4He | $1.3 \times 10^{17}$ |
| | or bubbles ∅ 0.7 | $2.0 \times 10^{16}$ |
| 205 | 2V–2(3)He | $3.6 \times 10^{16}$ |
| | 5V–2He | $1.2 \times 10^{17}$ |
| | or bubbles ∅ 2.4 | $2.7 \times 10^{16}$ |
| 330 | 2V–2(3)He | $3.4 \times 10^{16}$ |
| | Bubbles ∅ 2.8 | $2.4 \times 10^{16}$ |
| 470 | 2V–2(3)He | $3.1 \times 10^{16}$ |
| | Bubbles ∅ 3.8 | $1.8 \times 10^{16}$ |
| *Immersion temperature 400 °C* | | |
| Initial | V | $2.2 \times 10^{17}$ |
| | 3V | $1.4 \times 10^{17}$ |
| 140 | 2V–2(3)He | $8.1 \times 10^{16}$ |
| | 5V | $2.8 \times 10^{16}$ |
| | or 10V–He | $2.4 \times 10^{16}$ |
| | or bubbles ∅ 7.0 | $0.2 \times 10^{16}$ |
| 270 | 2V–2(3)He | $3.7 \times 10^{16}$ |
| | bubbles ∅ 10.4 | $0.08 \times 10^{16}$ |
| 500 | 2V–2(3)He | $3.7 \times 10^{17}$ |
| | bubbles ∅ 5.8 | $1.1 \times 10^{16}$ |

Table 4
Helium bubbles evolution from electron microscopy data

| He$^3$ concentration (appm) | Bubble size (nm) | Bubble concentration (s m$^{-3}$) | Main fraction and its relative content |
|---|---|---|---|
| *Immersion temperature 350 °C* | | | |
| 73 | – | – | – |
| 205 | 1–3 | $1.0 \times 10^{16}$ | 1 nm, 70% |
| 330 | 1.5–5.5 | $1.3 \times 10^{16}$ | 3 nm, 55% |
| 470 | 1–3 | $9.6 \times 10^{16}$ | 1 nm, 80% |
| *Immersion temperature 400 °C* | | | |
| 140 | $\leqslant 1$ | $<10^{15}$ | – |
| 270 | $\sim 8$ | $\sim 2 \times 10^{14}$ | – |
| 500 | 4–23 | $2.4 \times 10^{15}$ | 4 nm, 70% |

Table 5
Ultimate tensile strength ($\sigma_u$), yield stress ($\sigma_{0.2}$) and elongation ($\delta$) evolution

| He$^3$ concentration (appm) | $\sigma_u$ (MPa) | $\sigma_{0.2}$ (MPa) | $\delta$ (%) |
|---|---|---|---|
| *Immersion temperature 350 °C* | | | |
| Initial | 730 | 570 | 8.2 |
| 73 | 690 | 530 | 19.7 |
| 205 | 710 | 480 | 22.5 |
| 330 | 710 | 490 | 22.5 |
| 470 | 725 | 510 | 20.5 |
| *Immersion temperature 400 °C* | | | |
| Initial | 730 | 570 | 8.2 |
| 140 | 720 | 530 | 22.5 |
| | – | – | – |
| 270 | – | – | – |
| 500 | 740 | 560 | 25.0 |

is enclosed in these bubbles. As the He-3 content in the alloy increases, the bubble concentration and its size rise. The bubble distribution remains uniform through the grain volume.

The investigation of the V-1 alloy behavior in the D–T mixture under 400 °C has strengthened as a whole the earlier proposed mechanism for V-1 alloy structure changes. Some differences were observed due to the temperature increase from 350 up to 400 °C. The X-ray structure analysis showed that the boundary of the radiogenic helium solid solution range is shifted to higher He-3 contents.

The V-1 alloy lattice parameter peaked at a He-3 content of $\simeq$70 appm at 350 °C, but of $\simeq$270 appm at 400 °C. The maximum increase in lattice parameter was 0.07% at 350 °C and approximately twice higher (0.12%) at 400 °C.

Positron annihilation spectrometry revealed He–V cluster nucleation in the alloy within the solid solution range. The simplest cluster concentration (2V–2He and 2V–3He) peaked at a He-3 content of 140 appm up to $8 \times 10^{16}$ m$^{-3}$ and then decreased to $3.7 \times 10^{16}$ m$^{-3}$ at

270 appm and remained at this level at 400 °C exposure. The simplest cluster concentration at 350 °C exposure was constant in time ($\simeq 3.5 \times 10^{16}$ m$^{-3}$). As for more complex clusters, pure helium clusters were observed at 400 °C exposure: 5V and 10V–He ($2.4 \times 10^{16}$ m$^{-3}$) instead of helium rich clusters such as 5V–4He ($1.3 \times 10^{17}$ m$^{-3}$) at 350 °C exposure. The total He-3 content in the clusters was not higher than 8% at 350 °C and 2.4% at 400 °C exposure.

In our previous investigation of the V-1 alloy at 350 °C, helium bubbles were observed at the stage when radiogenic helium solid solution destruction took place. It was suggested that the bubbles were in the equilibrium state and He-3 pressure in the bubbles could be defined from the equation $p = 2\gamma/r$, where $\gamma$ is the surface tension and $r$ is the bubble size. The assumption of bubble equilibrium state was supported by microstructure investigations (no strain fields around bubbles were found). The calculation showed that the major amount of the formed helium was enclosed in the bubbles.

The distinguishing feature of the 400 °C exposure is the rare large-sized He-3 bubble formation within the helium solid solution region. The bubble size is anomalous large. During the process of the gradual destruction of the solid solution, the average size of the He-3 bubbles becomes similar to those observed at 350 °C exposure. This circumstance together with the presence of the large helium amount distributed in the lattice allows us to suggest that these bubbles are not equilibrium bubbles. It is possible to use the above equilibrium pressure equation only for the 505 appm He-3 content. The calculated helium amount enclosed in bubbles is $\simeq$60% of the total content in the alloy. About 200 appm He-3 still remains distributed in the lattice. This fact is in agreement with X-ray structure analysis data, which indicate that the reduction of the lattice parameter has not yet completed.

It is interesting to note that in the experiment on alpha-particle implantation in Pd–0.25Ag alloy at 300 °C the helium bubble formation was also observed at a He-3 concentration higher than 500 appm [15]. The bubble size was 3.3–3.5 nm. The bubble formation was observed at helium concentration about 200 appm in our 350 °C investigation. Rare bubble formation was observed at 140 appm helium under 400 °C exposure, but the equilibrium bubble fraction appears at a helium concentration of $\simeq$500 appm.

The tensile property evolution was in agreement with structure changes. After a slight decrease of the ultimate tensile strength and yield stress values due to annealing of the alloy, further slow strengthening and elasticity decrease took place. The ultimate tensile strength reduction at 400 °C was smaller than at 350 °C but the alloy elongation increased throughout the 400 °C exposure contrary to the 350 °C experiment where it peaked at a He-3 content of $\simeq$70 appm. These distinctions may be due to the more extensive width of the solid solution range and higher annealing rate of the alloy defect structure at 400 °C exposure.

## 5. Conclusion

The performed investigation revealed that structure changes of the V-1 alloy (Pd 15Ag 0.6Pt 0.6Ru 1.0Au 0.2Al) during the D–T exposure at 400 °C were similar to those at 350 °C. The main differences due to the temperature increase from 350 up to 400 °C were following:

- the radiogenic helium solid solution range was larger;
- the He–V cluster concentration within the solid solution range was twice higher and increased further up to an order of magnitude at 500 appm He-3;
- rare large-sized helium bubbles were observed within the solid solution range although the bubble size and its concentration became similar to those at 350 °C when the He-3 content run to 500 appm;
- the tensile property changes were less than at 350 °C.

The V-1 alloy did not loose its strength properties after tritium exposure under the performed investigation.

It is interesting to prolong the experiment up to a He-3 content in the alloy of 1000–1500 appm and to examine other palladium alloys, which are considered as a membrane diffuser material for a hydrogen isotope clean-up system.

## References

[1] A.N. Perevezentsev et al., Proceedings of the 5th Topical Meeting on Tritium Technology in Fission, Fusion and Isotopic Application, Italy, May 1995, Book of extended summaries, A-46.
[2] A.N. Perevezentsev et al., Proceedings of the 5th Topical Meeting on Tritium Technology in Fission, Fusion and Isotopic Application, Italy, May 1995, Book of extended summaries, A-15.
[3] J. Chabot et al., Proc. 18th SOFT, 2 (1994) 1067.
[4] V.V. Latishev, V.M. Bistritsky, Phys. Metalloved. 6 (1991) 5.
[5] V. Tebus et al., J. Nucl. Mater. 233–237 (1996) 1163.
[6] V. Tebus et al., Proc. 19th SOFT (1996) 1237.
[7] V. Tebus, L. Rivkis, et al., J. Nucl. Mater. 271&272 (1999) 345.
[8] P. Kirkegaard, N.J. Pedersen, M. Eldrup, Riso National Laboratory, RISO-M-2740, 1989.
[9] A. Seeger, Banhart, Phys. Stat. Sol. (a) 1 (N1) (1987) 171.
[10] H.E. Hansen, H. Rajainmaki, R. Talja, J. Phys. F: Met. Phys. 15 (1985) 1.

[11] K.O. Jensen, R.M. Nieminen, Phys. Rev. B 35 (1987) 2087.

[12] K.O. Jensen, M. Eldrup, B.N. Singh, M. Victoria, J. Phys. F. 18 (1988) 1069.

[13] K.O. Jensen, R.M. Nieminen, Phys. Rev. B 36 (1987) 8219.

[14] A.G. Zaluzny, U.V. Sokursky, V.N. Tebus, Heliy v Reactornih Materialah, Energoatomizdat, Moscow, 1988, p. 104.

[15] R. Lindau, A. Möslang, R.-D. Penzhorn, J. Nucl. Mater. 191–194 (1992) 178.